

Raman spectroscopy as a powerful analytical tool: probing the structure of matter

Tariq Jawhari

Unitat d'Anàlisi Molecular, CCiTUB, Universitat de Barcelona. Lluís Solé i Sabaris, 08028 Barcelona, Spain.

email: jawhari@ccit.ub.edu

Abstract. This article reviews the basic principles and instrumentation of Raman spectroscopy, discusses its advantages and limitations and gives examples of applications that illustrate the capabilities of the technique.

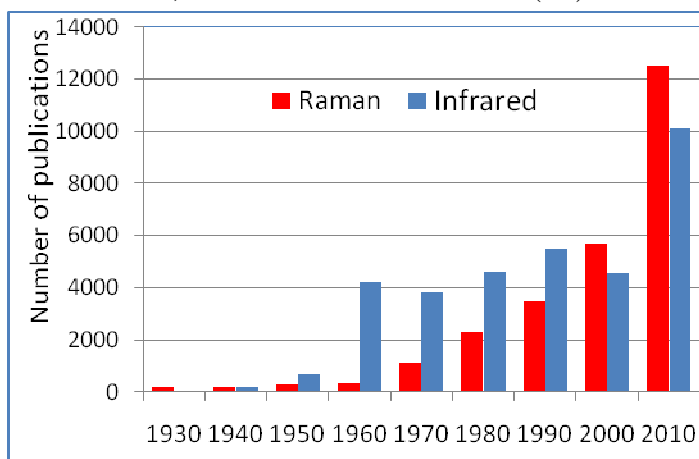
1. Introduction: some historical features

We shall see, in this contribution, the enormous possibilities that offer Raman Spectroscopy when identifying not only molecules but also in determining its structure and properties. So the obvious question that immediately arises is why, if Raman spectroscopy is such a powerful analytical technique, the method was for nearly half a century, mainly restricted to academic and research groups? Well, in fact, this is not totally exact: immediately after that Chandrasekhara Venkata Raman discovered in India in 1928 this new scattering effect, the method was enormously and uncommonly used during more than 10 years, founding the basis of molecular spectroscopy. Infrared spectroscopy (IR), the other fundamental molecular spectroscopy, which was discovered during the 19th century, was mainly restricted to some few laboratories due to some huge instrumental difficulties at this time. Soon after Raman published this new scattering phenomenon, obtained with a ridiculous simple experimental set-up[†], many groups over the world began to record Raman spectra: 58 publications appeared in the same year of the discovery and more than 2500 compounds were studied in less than 10 years!

However, this initial momentum of research stopped at the end of the 2nd World War when the first commercialized infrared spectrometers using photoelectric detectors were presented, as a result of an initiative of the US Government to produce a batch of infrared spectrometers for special government projects. During the next 20 years, Raman spectroscopy became a technique limited to some fundamental research in the academic world. The renaissance of Raman spectroscopy began in the sixties with the discovery of the laser: laser is the ideal source for Raman experiments since it provides highly intense monochromatic coherent radiation, with well defined polarization in a narrow non-diverging beam which can be focused to a diffracted limited spot. In the 70's, the typical Raman spectrometer consisted of a laser, a double-grating monochromator, which allows to diminish drastically the straight-light, and photo-multipliers tubes (PMT), which improve the detection of weak signals. In 1974, the first Raman microscope was presented separately in Lille (France) and at National Bureau of Standards (Washington).

During the last 25 years, the huge improvement made in instrumentation, mainly in compact air-cooled solid state lasers, holographic notch and edge filters to eliminate the strong laser line and high quantum efficiency and low-noise detectors such as charge-coupled devices (CCD), improved both the sensitivity and the simplicity of the Raman systems and opened the applications of Raman spectroscopy to many new fields of science. Raman spectroscopy which was basically known as a technique restricted to research labs, started to penetrate into the industrial world.

In the mid-80's, the first Fourier Transform (FT) Raman instruments began to appear in the



man and infrared shed over the last data obtained with arch program).

[†] The first experiment was obtained in February 1928 in Calcutta, using the sun as a source, a filter, a prism and the eyes as a detector. Two weeks later, the experiment was improved introducing an Hg-arc as a source and a photographic plate to record these new lines, in order to confirm these initial results, which were published in Nature on April 21 of the same year!!! Soon after Rutherford ranked the Raman effect as one of the best three discoveries in experimental physics in the decade and 2 years later, the Nobel's prize was conceded to Raman, the first Asian fellow to receive it.

market. Few years later, Raman instruments coupled with optical fibres, Raman mapping spectrometers and confocal Raman microscopes were offered. Nowadays both complex and large Raman instruments working with 4 or 5 lasers, in the ultraviolet (UV), visible and Near infrared (NIR) with a triple grating monochromator or very small miniaturized systems that can fit in a bag and can be used outdoor, are commercially offered. Finally, the evolution of Raman spectroscopy over the last 80 years can be followed, in table 1, by comparing the numbers of publications including “infrared” and “Raman” entries, respectively.

2. The Raman effect

When monochromatic radiation of frequency ν_0 is passed through a transparent medium, most of it is transmitted, some of it is absorbed and a small amount is scattered (less than 10^{-5} of the intensity of the exciting source). Most of this scattered light is at the same frequency as the incident radiation (called elastic or Rayleigh scattering) whilst a very small amount (10^{-3} to 10^{-4} of the Rayleigh intensity) is scattered at a frequency higher or lower than that of the incident radiation. It is this inelastic scattering that is referred as Raman Scattering.

Molecules are continuously vibrating. Both Raman and infrared spectroscopy detect and analyze the energy of the different vibrations that take place in the molecule, which will produce a spectrum. Every molecule or crystal has its own specific and unique Raman/IR spectrum. The way in which radiation is employed in Raman and infrared spectroscopy is different: in infrared spectroscopy a whole range of radiation, covering all IR spectrum, is directed onto the sample and absorption takes place when the frequency of the radiation matches precisely that of the vibration. In contrast, Raman spectroscopy uses a single frequency source to irradiate the sample and it is the scattered light from the molecule which is detected in the Raman experiment. The Raman scattering process can be easily explained by a simple quantum mechanical description (see figure 1): a photon of energy $h\nu_0$ colliding with a molecule can either be scattered elastically (Rayleigh)

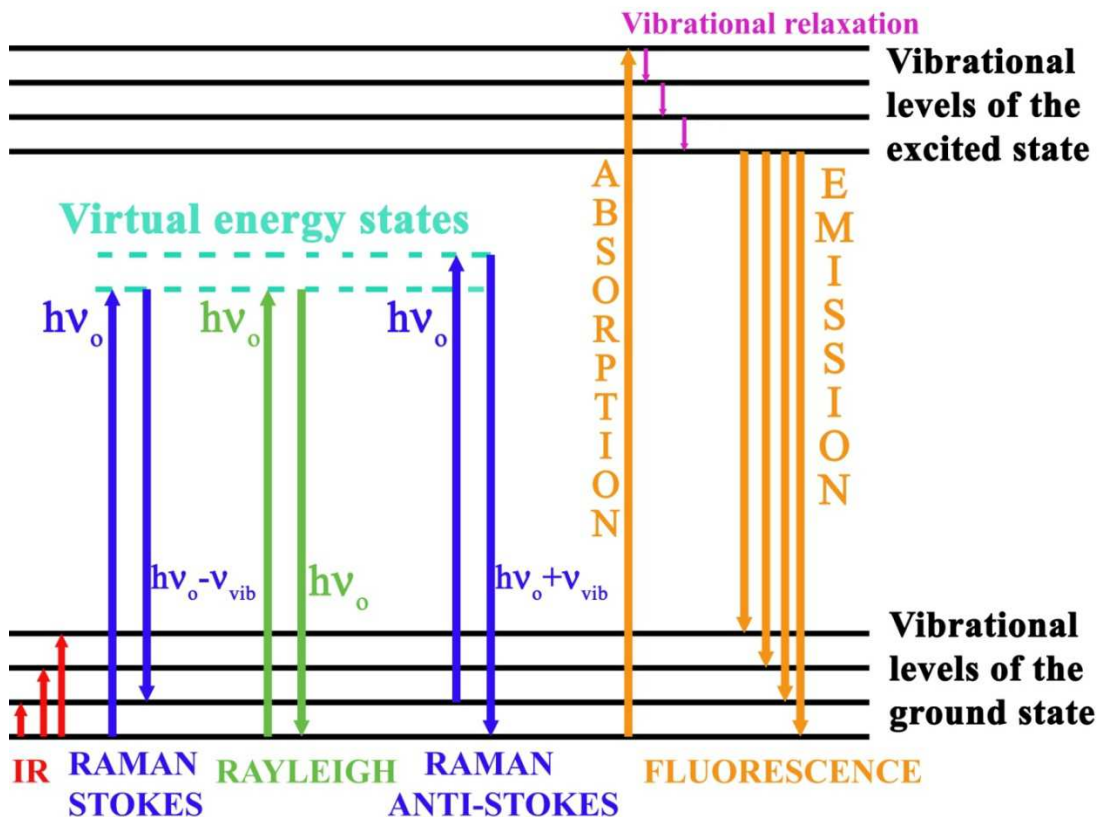


Figure 1: Vibrational and electronic energy-level diagram of a molecule showing the processes of IR absorption, Raman and Rayleigh scattering and fluorescence emission.

or inelastically (Raman). In the latter case, the collision with photons induces the molecule to undergo a transition between two vibrational energy levels of the molecule and the resulting scattered radiation has a different frequency than the incident photon. If during the collision, the molecule gains some energy $h\nu_{\text{vib}}$, the photon will be scattered at the frequency $h\nu_0 - h\nu_{\text{vib}}$, which is referred to as Stokes Raman scattering. Conversely, if the molecule loses some energy by relaxing from an excited vibrational level to the ground state, then the scattered energy will be at $h\nu_0 + h\nu_{\text{vib}}$, i.e. anti-Stokes Raman scattering[†]. Raman spectra are usually represented in wavenumbers shift (ν_{vib}), relative to the excitation line. The advantage of using such a shifted scale is that it allows working with a spectrum that gives directly the frequency of the molecular vibrations.

The relative intensities of the two processes depend on the population of the various states of the molecules, which is given by Boltzmann distribution. At room temperature, the probability to have molecules in an excited vibrational state is low, therefore anti-Stokes scattering will be weak compared to Stokes intensity, and will become weaker as the frequency of the vibration increases (see Figure 2). This is why the Raman spectrum is usually limited to the Stokes region. In some cases, both Stokes and anti-Stokes band intensities are measured in order to determine the temperature *in situ* at the microscopic level in some specific positions of the sample.

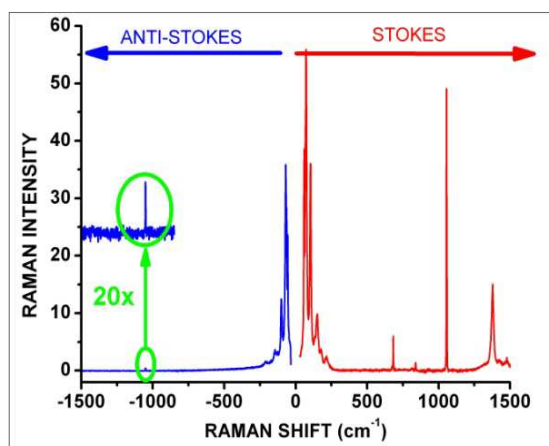


Figure 2: Stokes and anti-Stokes Raman spectra of cerussite (PbCO_3)

3. Instrumentation

Due to the immense technological advances in the last 20 years, many types of Raman instruments, from very large systems to miniaturized ones, working in different ranges of the spectrum, are found in the spectroscopy market. Very often, the difficulty for non specialist Raman users, is to decide what type of Raman instruments and conditions should be used for different kinds of samples or experiments. Basically, a Raman spectrometer is made of 4 main parts: a laser source, an optical system to illuminate the sample and collect the Raman signal, a “dispersive” system and a detector.

One of the most typical collecting systems is the so-called back-scattering geometry where the laser light is focused with the collection lens onto the sample and the scattered Raman collected by the same lens system and sent to the entrance slit of the spectrometer. Another possibility is to recollect the scattered light at 90° . The Raman microscope is a special back-scattering illumination-collecting system, where a typical optical microscope is used to both visualize and focalize the laser onto a microscopic region of the sample and to recollect the Raman signal. The dispersive system, which is a fundamental part of the spectrometer since it discriminates the weak Raman scattering from the intense laser line, is usually formed of several holographic gratings. Nowadays, the CCD is the typical detector used for Raman spectrometers. These detectors are often cooled at liquid nitrogen temperature in order to decrease the noise permitting therefore the detection of very weak signals.

More compact systems and miniaturised Raman instruments use filters technology with only one short focal length grating, often combined with optical fibres. These much cheaper instruments,

[†]During his studies on fluorescence in the mid-19th century, Sir G. Stokes postulated that the wavelength of a radiation emitted through a process of fluorescence is always higher than the excitation source wavelength. By analogy, the Raman lines are named Stokes and Anti-Stokes.

have a lower spectral resolution but are much more robust, easy to use and can be truly portable (i.e. dimension as low as 4"x2"x2").

Another type of Raman instrument is the Fourier Transform FT-Raman system, which uses the Michelson interferometer, instead of a dispersive unit, with a NIR source and an InGaAs detector [1]. FT-Raman and FTIR instruments can be very easily coupled which allow getting, with a unique system, a complete vibrational description of materials.

Nowadays, Raman microscopy is a very demanded and popular technique and most of the spectrometers proposed on the market are now furnished with an optical microscope. Such evolution is probably explained by the great advantage that the micro-Raman method offers to the microspectroscopist: it is possible to look at extremely small samples and get structural information at the submicrometric level. In fact, Raman microscopy is the method that offers the highest spatial resolution (both lateral and axial) of all molecular spectroscopies.

4. Advantages and limitations of Raman spectroscopy

4.1. Advantages

Raman spectroscopy is a practical method that offers a large series of advantages:

- No sample preparation; all types and sizes of samples can readily be analyzed as received.
- Very high spatial resolution ($\approx 0.5\mu\text{m}$) and very little sample required ($\approx 10^{-9}$ l or $\approx 10^{-12}$ g).
- Glass does not interfere with Raman spectrum thus traditional optics are suitable for Raman spectroscopy; simple accessories can be easily adapted for Raman measurements such as temperature and pressure cells, reactors for in-situ experiments, optical fibres for remote analysis.
- Common glass recipients such as vials or capillary tubes are used for solids, powder, liquids and gases. Plastics, quartz and even amber container, that can be sealed, can be utilized.
- Raman spectrum of water is weak which allows vibrational studies of aqueous solutions.
- The whole vibrational spectrum from 5 cm^{-1} to 4500 cm^{-1} is readily obtained which gives both information of the lattice modes at very low frequencies and internal modes.
- Standard Raman systems now offer the possibility to record both Raman and photoluminescent measurements in the UV, visible and near-infrared.
- Raman bands are usually well defined and resolved and the baseline is quite flat (if no fluorescence occurs) which makes the technique very powerful for structural characterization.
- Raman intensity is proportional to concentration therefore quantitative analysis is relatively simple.
- The possibility to couple optical fibres to Raman spectrometers has been largely used for remote in-process control and monitoring especially in industrial plants where the quality control laboratory is often separated from the process line.

4.2. Drawbacks

Basically, Raman spectroscopy has only one major limitation, but it is of considerable matter: Raman scattering is extremely weak[†]! As a result, the technique was known to be a complicated method when analyzing low concentration mixtures (below 1%) and material that fluoresces or samples with fluorescing impurities, since the large fluorescence background will strongly interfere with Raman signal. Fortunately, the new Raman systems with several laser sources permit to avoid fluorescence. Further, the recent technological developments of methods that increase the efficiency of Raman signal such as Raman resonance or surface enhanced Raman spectroscopy (SERS) have been successfully applied to detect and identify traces of chemical contaminants.

[†]Raman scattering cross section $\sim 10^{-31}\text{ cm}^2$; Infrared absorption cross section $\sim 10^{-18}\text{ cm}^2$; Fluorescence cross section $\sim 10^{-15}\text{ cm}^2$

5. Applications of Raman spectroscopy

In this part we shall review the different types of information on the microstructure and physical parameters of the condensed matter that can be obtained from the Raman spectrum:

5.1. Frequency

The frequency of the Raman band depends on the masses and positions of the atoms, the interatomic forces (i.e. force constants of the bonds) and the bond length. Therefore, any effects altering these features will produce a change in the frequency of the band. For instance, this is the reason why the band position is sensitive to the presence of stresses or strains: a tensile stress will determine an increase in the lattice spacing and, hence, a decrease in the wavenumber of the vibrational mode. In the case of compressive strain, the decrease of the lattice parameter yields a corresponding increase of the vibrational frequency. If the deformation of the structure follows an elastic behaviour, the shift will vary linearly with the magnitude of the stress, and as a result, the position of the Raman band can be used to measure the stress. It is well known that sharp Lorentzian band at 520 cm^{-1} of the first order Raman spectrum of crystalline silicon is quite sensitive to the presence of stress. For a biaxial stress in elastic regime, the stress ϵ in silicon can be obtained from

$$\epsilon = 250 \Delta\nu \text{ Mpa/cm}^{-1},$$

where $\Delta\nu$ is the Raman shift in wavenumber. Since the fabrication processes of semiconductor devices often produce strains in some localized microscopic regions, the Raman microprobe was found very useful in analyzing these micro-domains. This technique is now recognized as a powerful tool in identifying stress and strain in polycrystalline silicon structures used for the fabrication of large polysilicon micromechanical structures. These micromechanical systems based on surface-micromachining technologies can have serious stress effects that can cause mechanical device failure, curling or fracture, therefore, the micro-Raman system can be used as a quality control method and to improve several technological parameters.

Further, the presence of crystalline disorder also produces changes in the frequency of the band, usually towards lower wavenumbers. These are related to the breaking of translational symmetry in the crystal, which can be due to structural defects such as grain boundaries in nanocrystalline materials or dislocations. The position and shape of the Raman band can be simulated with a correlation length model [2] which allows to estimate the value of the correlation length L . L is defined as the characteristic size of crystalline domains where the translational symmetry of the crystal holds, and is related to the average grain size for nanocrystalline materials or to the average distance between defects for damaged crystals.

The presence of chemical impurities in the crystalline network may also give rise to changes in the mass of the atoms in the lattice sites which will shift the phonon frequency. For example, the presence of Ge atoms at substitutional positions in the silicon network produces a decrease in the frequency of the vibrational modes, due to a higher mass. This is known as the chemical effect and it has been used to characterize heteroepitaxial layers. For instance, the Raman spectrum of a typical SiGe_x alloy, as shown in Figure 3, presents three main bands, related to Si-Si, Si-Ge and Ge-Ge vibrational modes. The wavenumber of these modes follows a linear relationship with both chemical composition and strain [3]:

$$\nu_{\text{Si-Si}} = 520 - 68 x - 830 \sigma$$

$$\nu_{\text{Si-Ge}} = 500.5 + 14.2 x - 575 \sigma$$

$$\nu_{\text{Ge-Ge}} = 282.5 + 16 x - 384 \sigma$$

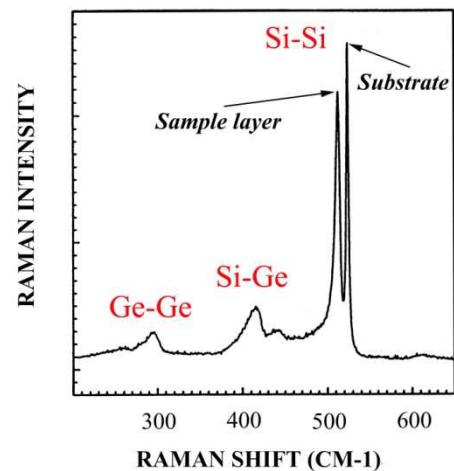


Figure 3: Raman spectrum of $\text{SiGe}_{0.3}$

where ν is the wavenumber of the Raman mode, x the chemical composition and σ the strain parallel to the substrate. Using these relationships, a single Raman spectrum of SiGe_x allows the determination of silicon and germanium contents as well as strain. Similar relationships have also been proposed for SiC_y as well as for more complex SiGe_xC_y and SiGe_xB_y ternary alloys [4].

5.2. Raman bandwidth

Raman bandwidth and bandshape are closely related to the crystalline order. In principle the bandwidth is related to the lifetime of the phonons. The presence of crystalline disorder produces a decrease of the phonon lifetime which thus generates an increase of the bandwidth. Therefore the density of defects can be evaluated from the bandwidth.

On the other hand, the bandshape of the Raman line is also affected by confinement of phonons being that given by the correlation length model [2]. This model allows the estimation of both the correlation length L and the average stress. This is interesting when studying nanocrystalline materials since the average grain size is given by L . The main limit for this measurement is that phonon confinement only occurs for sizes in the nanometric range ($L < 20\text{nm}$ for silicon). The changes in the bandshape and position of the Raman band related to phonon confinement permits the assessment of the average grain size and stress in nanocrystalline Si layers [5], as well as the density of defects in highly damaged Si films [6]. Figure 4 shows the spectra simulated for Si assuming spherical confinement and different values of the correlation length.

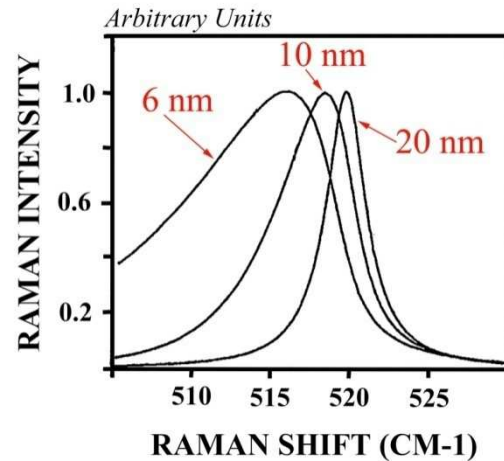


Figure 4: Simulation of silicon first order phonon mode assuming a spherical confinement L of 6 nm, 10 nm and 20 nm, respectively.

5.3. Raman intensity

The intensity of the Raman band is also very sensitive to the structure of crystals and as a result significant information can be obtained from intensity measurements. Damage in the lattice leads to a decrease of the intensity of the Raman modes, related to the breaking of bonds and changes in atomic forces displacements, and, hence produces a decrease of the Raman polarizability tensors. For instance, typical ion bombardment during doping process will alter the original crystal with a consequent reduction of the Raman signal intensity. The measurement of the Raman band intensity has therefore been applied to quantify the residual damage in processed wafers, such as ion implanted structures. Figure 5 shows an example on the quantification of the implanted induced damage in wafers of 6H-SiC (a hexagonal polytype of SiC) implanted with different doses of Ge^+ ions [7]. This is determined through the normalised intensity $I_n = (I_0 - I) / I_0$, where I is the intensity of the Raman band measured in the implanted layer and I_0 is the intensity of the Raman band measured in a virgin non-processed sample. For a low degree of damage, I is very similar to I_0 and I_n is close to 0. As damage increases, I decreases and I_n tends to the maximum value of 1. This last value gives a 100% of

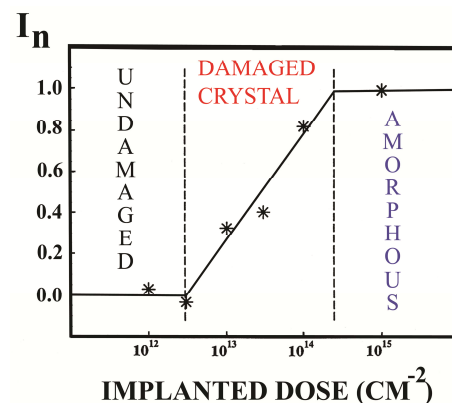


Figure 5: Relative micro-Raman intensity of the Longitudinal Optical mode of 6H-SiC versus the implantation dose

damage which corresponds to the damage level for which fully amorphization of the implanted layer occurs. In this case, all the crystalline modes vanish from the spectrum, and I becomes 0. This method permits to check the degradation of the crystalline structure and is also used for optimizing annealing process after ion implantation in order to eliminate the induced damage.

Intensity measurement is also performed for quantitative analysis of different polymorphisms, defects, disorder, micro-inhomogeneities, etc. Micro-Raman mapping measurements can also be carried out in order to determine, in a non destructive and simple way, the thickness and structural uniformity of thin films, such as cobalt silicide films (CoSi_2) deposited on Si used for IR detectors technology [8]. This was obtained by measuring the intensity of the Raman signal from the Si substrate at different points on the surface. As can be seen in Figure 6, the intensity of the Raman line of the substrate decreases in an exponential way, as the thickness of the layer increases. This is due to absorption of light in the layer. This method allows detection of CoSi_2 films as thin as 3-4 nm, and the CoSi_2 film thickness can be measured in the range between 10 and 100 nm with an uncertainty below 10%. More applications of Raman microspectroscopy on semiconducting materials can be found in Refs. [9-11].

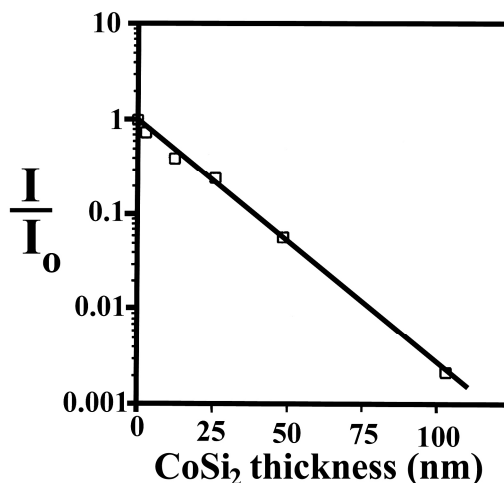


Figure 6: Relative Raman intensity of the 1st order Si mode in function of CoSi_2 layer thickness.

Crystalline transformation degree

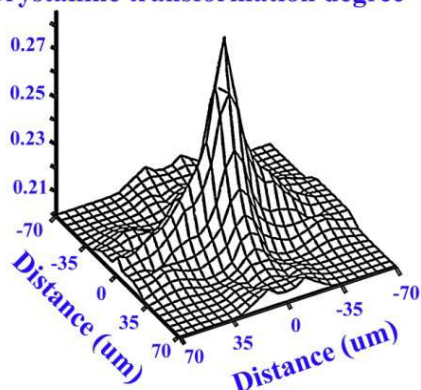


Figure 7: three-dimensional map showing the variation of the crystalline transformation degree along the Vickers micro-indentation.

strength of materials, it remains one of the least fundamentally understood mechanical-analysis methods. The main reason for the lack of information about the process of deformation during the application of an indenter in a material is the difficulty of detecting experimentally the effects of the process of microindentation inside and around the impression. Micro-Raman spectroscopy is one of the few methods that enable to analyze structural changes along the microindentation without requiring any sample preparation that would alter the microstructure in the zone of interest. PVF_2 presents a crystalline transformation, from the non planar (TGTG') conformation [form II(α)] to the planar zigzag (TTTT) structure [form I(β)], that is sensitive to the degree of stress submitted to the sample. The crystal transformation from II(α) to form I(β) can be followed by measuring the intensity of the two bands at 799 and 840 cm^{-1} , respectively, and the relative degree of crystalline modification is given by the coefficient $R = 100 I_{840\text{cm}^{-1}} / (I_{840\text{cm}^{-1}} + I_{799\text{cm}^{-1}})$. Raman mapping of the microdeformed zone produced by Vickers indenter microhardness techniques in PVF_2 (see Figure 7) reveals the

existence of three zones which appear to depend on the elastoplastic behaviour of the material and on the type of deformation to which the material is subjected, mainly determined by the geometry of the indenter [13].

Micro-Raman analyses of the transition front in the neck region of stretched polymers have also been carried out [15-16]. The change in the crystalline structure that takes place in the transition front between the isotropic and oriented regions in uniaxially cold drawn PVF₂ can readily be followed by Raman micro-spectroscopy. The Raman mapping of the transition region allows to provide the distribution of crystalline phase transformation along the neck (see Figure 8). Further, micro-Raman polarized measurements carried out along the neck region in uniaxially stretched polypropylene allowed to determine the evolution of the polymer chain orientation along the transition zone as a function of the drawing rates, which was correlated with other parameters associated with the drawing response of these polymers [16].

Raman microscopy was found to be a powerful technique in the identification of multilayer polymer structures [17], which are commonly used as food packaging containers, and in some cases to probe the quality of the adhesion between layers. The whole operation just takes some few minutes since no sample preparation is needed: the different layers are easily characterized after having cut the multilayer with a typical razor blade and holding it under the microscope objective with an ordinary clip. Micro-Raman spectroscopy is also a very helpful technique in characterizing different morphological features and micro-damaged or degradation in some localized region of materials[9]: for instance, Figure 9 shows the transmitted crossed polarized

light micrograph of polymeric composite interface between a fibre of polyethylene terephthalate (PET) and polypropylene (PP) matrix, which allows the visualization and location of two different morphologies, i.e. the transcrystalline zone near the fibre and the typical spherulitic structure away of the interface. In this example, combining transmitted crossed polarized light microscopy with micro-Raman spectroscopy allows to get information on the different types of polymer chains orientation that prevail in each of the two different morphological species. Further, the use of polarized Raman microscopy with polarized light microscopy enabled the characterization of the banded structures that are often observed in the spherulites of polymers. The evolution of the lamellae orientation along the periodical ring pattern structure observed in the crossed polarized micrograph was determined by exploiting the high resolving power of the micro-Raman instrument.

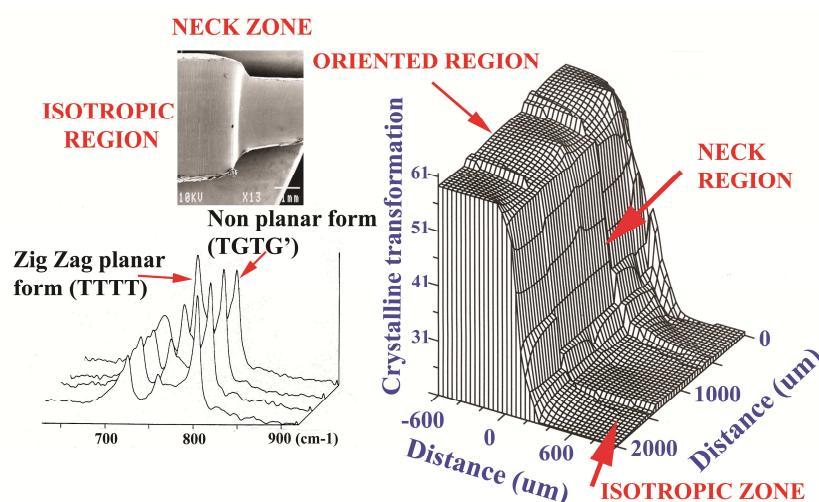


Figure 8: Raman mapping of the neck region of uniaxially cold drawn PVF₂.

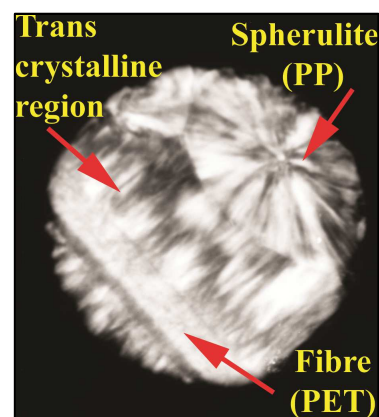


Figure 9: Crossed polarized optical micrograph of a polymeric composite

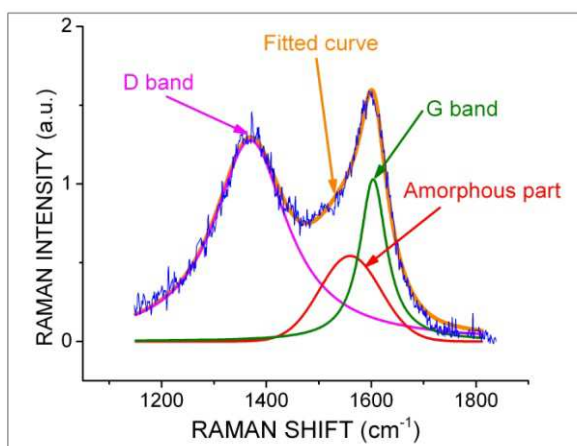


Figure 10: Curve-fitting of black carbon Raman spectrum

with a Lorentzian shape, at 1370 and 1603 cm^{-1} , respectively, and a broader Gaussian feature centered at about 1550 cm^{-1} assigned to amorphous graphitic phase. The Raman analysis shows that this material has a high degree of disorder and consists principally of non-hydrogenated sp^2 carbon bonds [18]. The microcrystalline planar crystal size was also determined from the following relationship:

$$L_a = [I(D)/I(G)]^{-1},$$

where $I(D)$ and $I(G)$ are the integrated intensities of the D and G bands, respectively. The sample analyzed here has a low microcrystalline planar size, i.e. L_a is of the order of 2 nm. Since Raman spectrum of carbons is sensitive to its microstructure, Raman spectroscopy is a very valuable method in characterizing new synthesized carbons-based materials such as fullerenes, graphenes, fullerites, nanotubes, carbon fibers, layered intercalate carbon-based structures, etc. [19-23]. Further, Raman spectroscopy can give some valuable information on doping, temperature and pressure response in C60 and C70, allows to identify MWCNT (multi-wall carbon nanotubes) and SWCNT (single-wall carbon nanotubes), to determine directly the stress, strain as well as diameter size of carbon nanotubes, and finally to find out the number of graphene layers.

Geologists have been particularly interested in laser Raman microspectroscopy as a mean of nondestructive analysis of single fluid inclusions. Fluid inclusions are multiphase systems of

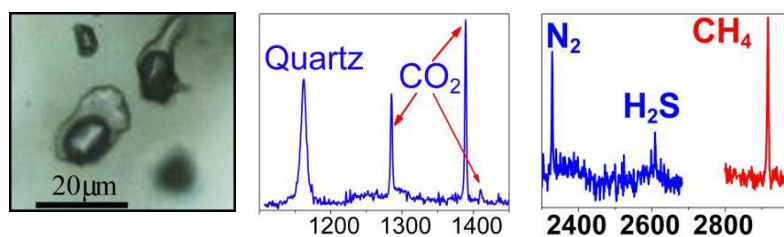


Figure 11: Raman spectra of a microinclusion in quartz.

minuscule volumes (tens of cubic micrometers) - often with coexisting liquid, gaseous or solid phases - trapped within a mineral host. The coupling of Raman microscopy with microthermometry is still the only viable option to obtain the composition of individual fluid inclusions. For example, Figure 11 shows the Raman spectra of a liquid and vapour phase inclusion in a quartz matrix. Due to the complex histories of many geological environments, individual minerals may contain several generations of fluid inclusions which are a direct source of information on the initial environment of rock and their subsequent geological history. The chemical analysis of fluid inclusions provides important data related to many mineralogical, geochemical and geological processes. In gemology, Raman is now commonly used for the detection of jewels treatments and the analysis of the nature and identification of gemstones.

Raman spectroscopy was found very useful for process monitoring both in industrial plants and quality control laboratory. For example, it was applied to thin film chalcopyrite photovoltaic

technologies: Raman modes from the chalcopyrite layers are very sensitive to features related to their crystalline quality, chemical composition and the presence of secondary phases that are relevant for the optoelectronic properties of the absorbers and the efficiency of solar cells [24-25]. Measurements performed at different process steps allow for the monitoring of the synthesis process of the chalcopyrite layers, giving information directly related to their processing conditions. Experimental configurations have been successfully applied for the monitoring at on-line and in-situ real time levels of the electro-deposition processes involved in the fabrication of low-cost electrochemical based chalcopyrite solar cells [26].

At low frequencies, the lattice modes corresponding to intermolecular collective vibrations and semi-internal motions associated to the rotation of groups of atoms within the molecule, are easily detected with a Raman spectrometer. These modes are very sensitive to polymorphic structures and have been largely used in the pharmaceutical analysis to characterize pharmaceutical solid-state transformations, such as amorphization, crystallization, hydrate formation/dehydration, co-crystal formation, etc.

During the last two decades, Raman spectroscopy has been widely used in the field of Art and Archeology, in collaboration with conservation scientists, art historians, archaeologists, and applied to the study of pigments in manuscripts and artwork, textiles, enamels, mummies, bio-deteriorated wall paintings, resins, ivories etc. The technique can be utilized to date artwork and even to establish forgery and frauds. Also, a procedure was proposed to determine in a non destructive way the colour printing order in multilayer artistic prints [27].

More recently, Raman spectroscopy has become a useful analytical tool in biomedical science to differentiate between healthy and diseased tissues. The method generates information about the molecular composition, molecular structures, and molecular interactions in a cell and tissue. Raman spectroscopy provides a measure of biologically important molecular group such as lipids, proteins and nucleic acids since most of these molecules are Raman actives and their spectra can be considered as specific fingerprints. As the transformation from normal to cancerous tissues is characterized by molecular changes of tissues constituents, these variations should be reflected in the Raman spectra and can be used as phenotypic markers of the disease. The monitoring of these molecular changes within the tissues can provide diagnostic and prognostic information for early detection of tumour. Indeed, Raman spectroscopy was proposed as a diagnostic method, complementary to histopathology or immunochemistry. Now, the ultimate objective in cancer research is the replacement of biopsy with fiber-optic Raman spectroscopy.

References

- [1] Ellis G., Hendra P.J., Hodges C., Jawhari T., Jones C., Le Barazer P., Passingham C., Royaud I., Sanchez-Blasquez A., Warnes G. 1989 *The Analyst* **114** 1061
- [2] Fauchet P.M., Campbell H.I. 1988 *CRC Crit. Rev. Solid State Mater. Sci.* **14** S79
- [3] Tsang J.C., Mooney P.M., Dacol F., Chu J.O. 1994 *J. Appl. Phys.* **75** 8098
- [4] Pérez-Rodríguez A., Romano-Rodríguez A., Cabezas R., Morante J.R., Jawhari T., Hunt C.E. 1996 *J. Appl. Phys.* **80** 5736
- [5] Achiq A., Rizk R., Gourbilleau F., Madelon R., Garrido B., Pérez-Rodríguez A., Morante J.R., 1998 *J. Appl. Phys.* **83** 5797
- [6] Macía J., Martin E., Pérez Rodríguez A., Jiménez J., Morante J.R., Aspar B., Margail J. 1997 *J. Appl. Phys.* **82** 3730
- [7] Pérez-Rodríguez A., Pacaud Y., Calvo-Barrío L., Serre C., Skorupa W., Morante J.R. 1996 *J. Electr. Mater.* **25** 541
- [8] Pérez-Rodríguez A., Roca E., Jawhari T., Morante J.R., Schreutelkamp R.J. 1994 *Thin Solid Films* **251**, 45
- [9] Jawhari T. 1995 *Handbook of Advanced Materials Testing*, Marcel Dekker, New York
- [10] Jawhari T., Pérez-Rodríguez A. 1999 *The Internet Journal of Vibrational Spectroscopy*,

II(4)

- 41 (<http://www.ijvs.com/volume2/edition4>)
- [11] Jawhari T. 2000 *Analisis* **28** 15
- [12] Jawhari T., Merino J.C., Pastor J.M. 1992 *J. Mater. Sci.* **27** 2231
- [13] Jawhari T., Merino J.C., Rodriguez-Cabello J.C., Pastor J.M. 1993 *Polym.* **34** 613
- [14] Jawhari T., Merino J.C., Pastor J.M. 1992 *J. Mater. Sci.* **27** 2237
- [15] Jawhari T., Merino J.C., Rodriguez-Cabello J.C., Pastor J.M. 1992 *Polym. Comm.* **33** 4199
- [16] Pastor J.M., Jawhari T., Merino J.C., Fraile J. 1993 *Makromol. Chem. Macromol. Symp.* **72** 131
- [17] Jawhari T., Pastor J.M. 1992 *J. Mol. Struct* **266** 205
- [18] Jawhari T., Roig A., Casado J. 1995 *Carbon* **33** 1561
- [19] Afanasyeva N.I., Jawhari T., Klimenko I.V., Zhuravleva T.S. 1996 *Vibrat. Spectrosc.* **11** 79
- [20] Klimenko I.V., Zhuravleva T.S., Jawhari T. 1996 *Synth. Met.* **86** 1
- [21] Afanasyeva N.I., Belogorokhov A.I., Blank V.D., Jawhari T., Ovchinnikov A.A. 1997 *Macromol. Symp.* **119** 207
- [22] Klimenko I.V., Zhuravleva T.S., Afanasyeva N.I., Jawhari T. 1996 *Polym. Sci.* **A12** 1336
- [23] Klimenko I.V., Zhuravleva T.S., Geskin V.M., Jawhari T. 1998 *Mater. Chem. Phys.* **56(1)** 14
- [24] Rudigier E., Pietzker Ch., Wimbor M., Luck I., Klaer J., Scheer R., Barcones B., Jawhari T., Alvarez-Garcia J., Perez-Rodriguez A., Romano-Rodriguez A. 2003 *Thin Solids Films* **431** 110
- [25] Rudigier E., Barcones B., Luck I., Jawhari T., Perez-Rodriguez A., Scheer R. 2004 *J. Appl. Phys.* **95** 5153
- [26] Izquierdo-Roca V., Saucedo E., Jaime-Ferrer J.S., Fontané X., Pérez-Rodríguez A., Bermúdez V., Morante J.R. 2011 *J. Electrochem.Soc.* **158** 521
- [27] Vila A., Jawhari T., García J.F 2007 *J. Raman Spectrosc.* **38** 1267